# Quantitative $^{99m}$Tc-MDP SPECT/CT as an alternative to $^{18}$F-NaF PET/CT for objective assessment of osteoblastic bone metastases

**Nazim Coskun[1] MD,**
**Berkay Cagdas[1] MD,**
**Nilufer Yildirim[1,2] MD**

*1. Ankara City Hospital, Department of Nuclear Medicine, Ankara, Turkey*
*2. Ankara Yildirim Beyazit University, Department of Nuclear Medicine, Ankara, Turkey*

*Keywords:* PET/CT - SPECT/CT - SUV - Bone metastasis

***Corresponding author:***
Nazim Coskun MD,
Ankara Sehir Hastanesi,
Nukleer Tip Klinigi, Universiteler Mah, 06800, Cankaya, Ankara, Turkey
Tel: +90 312 552 6000
nazim@coskun.co

*Received:*
19 May 2022
*Accepted revised:*
30 May 2022

## Abstract

**Objective:** To investigate the correlation between the standardized uptake value (SUV) metrics derived from technetium-99m ($^{99m}$Tc) methylene diphosphonate (MDP) single photon emission computed tomography/computed tomography (SPECT/CT) and fluorine-18 ($^{18}$F) sodium fluoride (NaF) positron emission tomography (PET)/CT. **Subjects and Methods:** A total of 129 metastatic lesions from 14 patients who underwent both $^{99m}$Tc-MDP SPECT/CT and $^{18}$F-NaF PET/CT within one month were included in the analyses. The lesions with markedly increased uptake were semi-automatically segmented into a volume of interest in both SPECT and PET images by taking the 42% of maximum uptake as a threshold. Maximum, average and minimum SUV (namely, SUVmax, SUVmean and SUVmin) were recorded for each lesion. The strength of correlation was evaluated with Pearson's correlation analysis. **Results:** The correlation coefficitients for SUVmax, SUVmean and SUVmin derived from SPECT and PET images were 0.652, 0.653 and 0.635, respectively (all P<0.001). Lesions with a volume of at least 5cm$^3$ demonstrated a stronger correlation, increasing the correlation coefficients to 0.714, 0.724 and 0.686, respectively (all P<0.001). The strongest correlation was seen in the lesions of the appendicular skeleton, with coefficients for SUVmax, SUVmean and SUVmin being 0.769, 0.791 and 0.761, respectively (all P<0.001). **Conclusions:** The SUV metrics derived from $^{99m}$Tc-MDP SPECT/CT strongly correlate with $^{18}$F-NaF PET, especially for relatively large lesions located in the appendicular skeleton. Technetium-99m-MDP SPECT/CT could potentially be used as an alternative method to $^{18}$F-NaF PET/CT for quantitative evaluation and objective follow-up of bone metastases.

*Hell J Nucl Med 2022; 25(2): 132-137* *Epub ahead of print: 3 August 2022* *Published online: 29 August 2022*

## Introduction

The demand for imaging-based patient follow-up in oncology has led to a paradigm shift in the interpretation of molecular imaging modalities like positron emission tomography (PET) and single photon emission computed tomography (SPECT). Today, rather than being evaluated with relative or semi-quantitative measures, absolute quantification of images is offered in terms of standardized uptake value (SUV). This expansion of quantifiable data has offered novel aspects for objective decision making and improved patient management, and thus, quantification has become a fundamental component of nuclear medicine workflow. To date, quantitative assessment has been restricted to PET imaging, while SPECT remained mostly on a qualitative or semi-quantitative level. Thanks to recent developments in gamma camera instrumentation and medical image analysis, it has become possible to perform quantitative SPECT by using common SUV metrics in SPECT/CT [1, 2].

Technetium-99m-methylene diphosphonate ($^{99m}$Tc-MDP) and fluorine-18-labeled sodium fluoride ($^{18}$F-NaF) are two different bone tracers with almost identical mechanisms of skeletal uptake. Methylene diphosphonate labeled with $^{99m}$Tc has been widely used in SPECT/CT imaging for the detection and follow-up of osteoblastic bone metastases ever since the introduction of integrated SPECT/computed tomography (CT) scanners in the late 1980s [3-5].The widespread availability of $^{99m}$Tc-MDP SPECT/CT as a cost-effective and safe modality has allowed for earlier diagnosis and treatment of osteoblastic bone metastases and has led to improved patient outcomes [6-8]. On the other hand, PET/CT imaging with $^{18}$F-NaF is a relatively new molecular imaging modality that was approved by the FDA in 2011. Fluorine-18-NaF PET/CT offers several advantages over $^{99m}$Tc-MDP SPECT/CT, such as higher spatial resolution and a shorter waiting period after injection [9,10]. Nevertheless, the availability of $^{18}$F-NaF PET/CT is limited to fewer centers and its high cost is a major downside. As a PET radiopharmaceutical, $^{18}$F-NaF already allows for absolute qu-

antification and the SUV metrics have been routinely incorporated in the PET-based assessment of osteoblastic bone metastases. Adopting a similar approach to the $^{99m}$Tc-MDP SPECT/CT workflow could improve the accessibility to quantitation of bone metastases and contribute to patient management.

In this context, we aimed to investigate whether SUV metrics derived from $^{99m}$Tc-MDP SPECT/CT correlate with those from $^{18}$F-NaF PET/CT and to evaluate whether quantification of $^{99m}$Tc SPECT/CT could be a substitute for $^{18}$F-NaF PET in the clinical practice.

## Subjects and Methods

### Study design

This retrospective observational study included all patients referred to our department between January 2021 and April 2022 who had metastatic bone lesions detected on $^{99m}$Tc-MDP SPECT/CT and underwent $^{18}$F-NaF PET/CT within one month after SPECT. Exclusion criteria were: 1) Receiving systemic or local therapies between SPECT and PET imaging, 2)The time between SPECT and PET being longer than one month, 3) The presence of disseminated bone involvement (e.g., super-scan) and 4) Inaccessibility of imaging and/or clinical data. Informed consent was obtained from all individual participants included in the study. The institutional ethics committee approved the study (Approval no: E2-22-1872).

### Study outcome

The primary outcome was to evaluate the strength of correlation between SUV metrics derived from $^{99m}$Tc-MDP SPECT and $^{18}$F-NaF PET on a lesion level.

### $^{99m}$Tc-MDP SPECT/CT protocol

A 16-slice CT-integrated dual-head gamma camera (GE Discovery NM/CT 670; GE Healthcare, Milwaukee, WI) was used for the SPECT/CT imaging. Each patient received 20mCi of $^{99m}$Tc-MDP and underwent whole-body planar imaging at 3 hours following radiotracer injection. After a whole-body scan, SPECT/CT fusion images were acquired by positioning the lesions with increased uptake within the field of view. The area with the most lesions was picked in case of multiple bone metastases. Axial slices were obtained by iterative reconstruction (ordered subset expectation maximization, 14 subsets, 6 iterations) with a slice thickness of 3.5mm. Gaussian smoothing (full-width at half maximum=5mm), attenuation correction and model-based scatter correction were applied to the SPECT images. The lesions showing markedly increased uptake with respect to background activity were semi-automatically segmented into a 3-dimensional volume of interest by taking the 42% of maximum uptake as a threshold. Segmentations were performed by two nuclear medicine physicians with 3 and 7 years of experience, using Q.Metrics software on GE AW Volume Share 7 workstation. Differences of opinion were resolved by reaching a consensus.

### Quantification of $^{99m}$Tc-MDP SPECT/CT

A planar acquisition of a flat source with known activity was previously performed. The total number of counts in the image of that source was measured to determine the sensitivity of the gamma camera, as suggested by the Committee on Medical Internal Radiation Dose [11]. Based on the sensitivity of the system, the reconstructed SPECT signal was converted from counts to activity concentration according to the formula:

$$\text{Activity (Bq/mL)} = 37\times10^{3}\times\frac{60}{\text{Sensitivity (cts/min/}\mu\text{Ci)}\times T\times \text{mL}}$$

where T is the duration of the scan in seconds. Then the SUV of each voxel within the VOI was calculated according to the formula:

$$\text{SUV} = \frac{\text{Activity in voxel}}{\text{Injected activity}}\times\text{Body weight (g)}$$

Maximum SUV, SUVmin and SUVmean, respectively corresponding to maximum, minimum, and average SUV within the volume of interest (VOI), were then recorded for each lesion.

### $^{18}$F-NaF PET/CT protocol

A 16-slice CT-integrated PET/CT scanner (GE Discovery IQ PET/CT; GE Healthcare, Milwaukee, WI) was used for PET imaging. Patients were intravenously injected with 370MBq (10mCi) $^{18}$F-NaF. Forty-five minutes later, non-contrast-enhanced whole-body CT (120kV, 10-90mAs) and PET (3 minutes per bed) images were acquired at a slice thickness of 3.5mm and reconstructed with Bayesian penalized likelihood algorithm (Beta: 350). The foci of increased uptake corresponding to those segmented in SPECT/CT were delineated into a 3D VOI with the same method used for SPECT segmentation (42% threshold). The same three SUV metrics (SUVmax, SUVmean and SUVmin) were recorded for the PET equivalent of each lesion segmented in $^{99m}$Tc-MDP SPECT/CT.

### Statistical analyses

Continuous variables were expressed as median (interquartile range) and categorical variables as frequency (percentage). The strength of correlation between SPECT and PET-based quantitative metrics was evaluated with Pearson's correlation analysis. Statistical analyses were performed using the R statistical package (R Foundation for Statistical Computing, Vienna, Austria) and Stata/MP 16 (Stata Corporation, College Station, Texas, USA) software. A P-value below 0.05 was considered statistically significant.

## Results

### Characteristics of lesions

A total of 129 lesions from 14 consecutive patients were in-

cluded in the final analyses. Six patients were under follow-up for prostate cancer and 8 for breast cancer. The median (interquartile range; IQR) age was 63 (57-72) years. The characteristics of the study population and metastatic bone lesions are depicted in Table 1. Ribs were the most frequent site of metastasis (n=36, 27.9%), followed by the spine (n=51, 39.5%). Most of the lesions were in the axial skeleton (n=93, 72.1%), and 36 (27.9%) were in the appendicular skeleton. The volume of the lesions varied between 0.5 and 28.8cm$^3$, with a median of 3.4cm$^3$. The median (IQR) number of lesions was 6 (4-13) per patient.

***Table 1.*** *Characteristics of the study population and metastatic bone lesions.*

| | **Patients (n=14)** |
|---|---|
| Age, *years* | 63 (57-72) |
| *Sex / Primary Tumor* | |
| Male / Prostate cancer | 6 (43%) |
| Female / Breast cancer | 8 (57%) |
| Body Mass Index | 27.5 (24.0-37.2) |
| | **Lesions (n=129)** |
| *Localization* | |
| Ribs | 51 (39.5%) |
| Spine | 36 (27.9%) |
| Pelvis | 14 (10.9%) |
| Scapula | 10 (7.8%) |
| Extremities | 9 (7.0%) |
| Sternum | 7 (5.4%) |
| Calvarium | 1 (0.8%) |
| Cartilage tissue | 1 (0.8%) |
| *PET SUV* | |
| SUVmax | 27.7 (15.3-36.2) |
| SUVmean | 16.2 (9.6-22.6) |
| SUVmin | 11.8 (6.5-15.4) |
| *SPECT SUV* | |
| SUVmax | 14.1 (9.3-21.1) |
| SUVmean | 8.6 (5.3-12.2) |
| SUVmin | 5.9 (3.7-8.8) |

*Data are presented as median (interquartile range) for continuous variables, and frequency (percentage) for categorical variables.*

### Overview of SUV metrics

The median (IQR) values of SUVmax, SUVmean and SUVmin were 14.08 (9.3-21.08), 8.63 (5.27-12.16), 5.88 (3.65-8.78), respectively, $^{99m}$Tc-MDP SPECT/CT, and 27.7 (15.29-36.22), 16.23 (9.58-22.61), 11.77 (6.52-15.4) in $^{18}$F-NaF PET/CT.

### Correlation between SUV of SPECT and PET

All three SUV variants showed strong positive correlation (Table 2). If all lesions were included in the analysis, the correlation coefficients for SUVmax, SUVmean and SUVmin were found as 0.652, 0.653 and 0.635, respectively (all P< 0.001). Lesions with a volume of at least 5cm$^3$ demonstrated a stronger correlation, increasing the correlation coefficients to 0.714, 0.724 and 0.686, respectively (all P<0.001).The strongest correlation was seen in the lesions of the appendicular skeleton, with coefficients for SUVmax, SUVmean and SUVmin being 0.769, 0.791 and 0.761, respectively (all P< 0.001). Figure 1 shows the dot plot and the regression line for SUVmax, according to size and location of lesions. Single photon emission tomography and PET images of a patient are presented in Figure 2.

***Table 2.*** *Correlation coefficients for SUV derived from $^{18}$F-NaF PET and $^{99m}$Tc-MDP SPECT according to the volume and localization of lesions (all P<0.001)*

| | **SUVmax** | **SUVmean** | **SUVmin** |
|---|---|---|---|
| All Lesions (n=129) | 0.652 | 0.653 | 0.635 |
| *Volume* | | | |
| <5cm$^3$ (n=84) | 0.639 | 0.639 | 0.625 |
| ≥5cm$^3$ (n=45) | 0.714 | 0.724 | 0.686 |
| *Localization* | | | |
| Axial (n=93) | 0.566 | 0.559 | 0.545 |
| Appendicular (n=36) | 0.769 | 0.791 | 0.761 |

## Discussion

This study has two messages. First, the SUV metrics derived from $^{99m}$Tc-MDP SPECT/CT strongly correlate with $^{18}$F-NaF PET, especially for relatively large lesions located in the appendicular skeleton. Second, this significant correlation implies that $^{99m}$Tc-MDP SPECT/CT could potentially be used as an alternative method to $^{18}$F-NaF PET/CT for quantitative evaluation and objective follow-up of bone metastases. Of note, the SUV derived from $^{99m}$Tc-MDP was relatively smaller than the SUV of $^{18}$F-NaF PET, which is a possible outcome of partial volume effect due to lower spatial resolution in SPECT imaging [12].

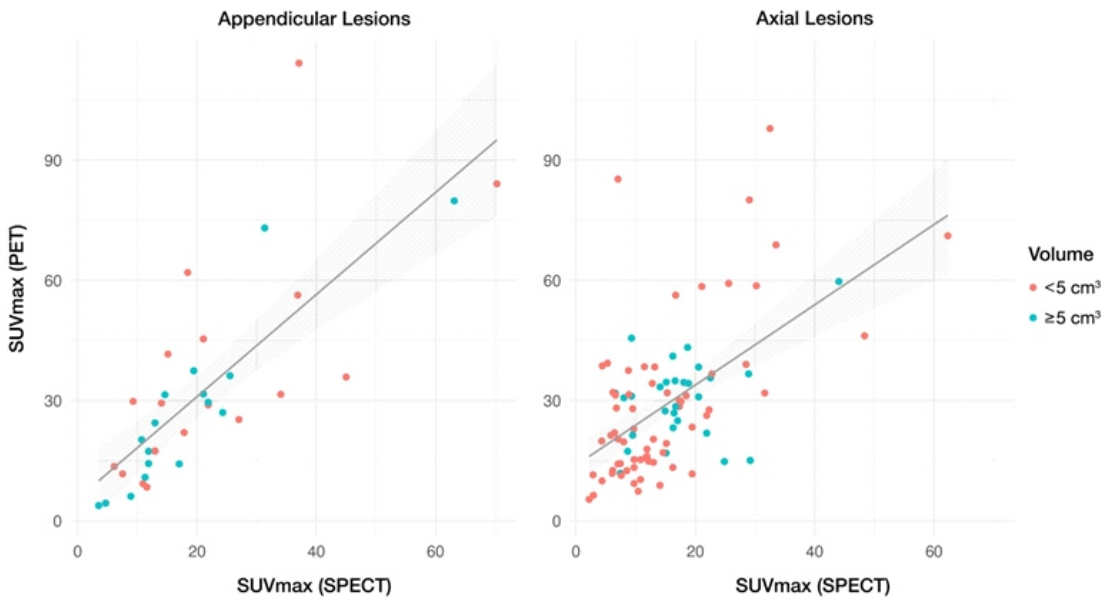


**Figure 1.** Scatter plots and regression lines of SUVmax according to the size and localization of lesions.

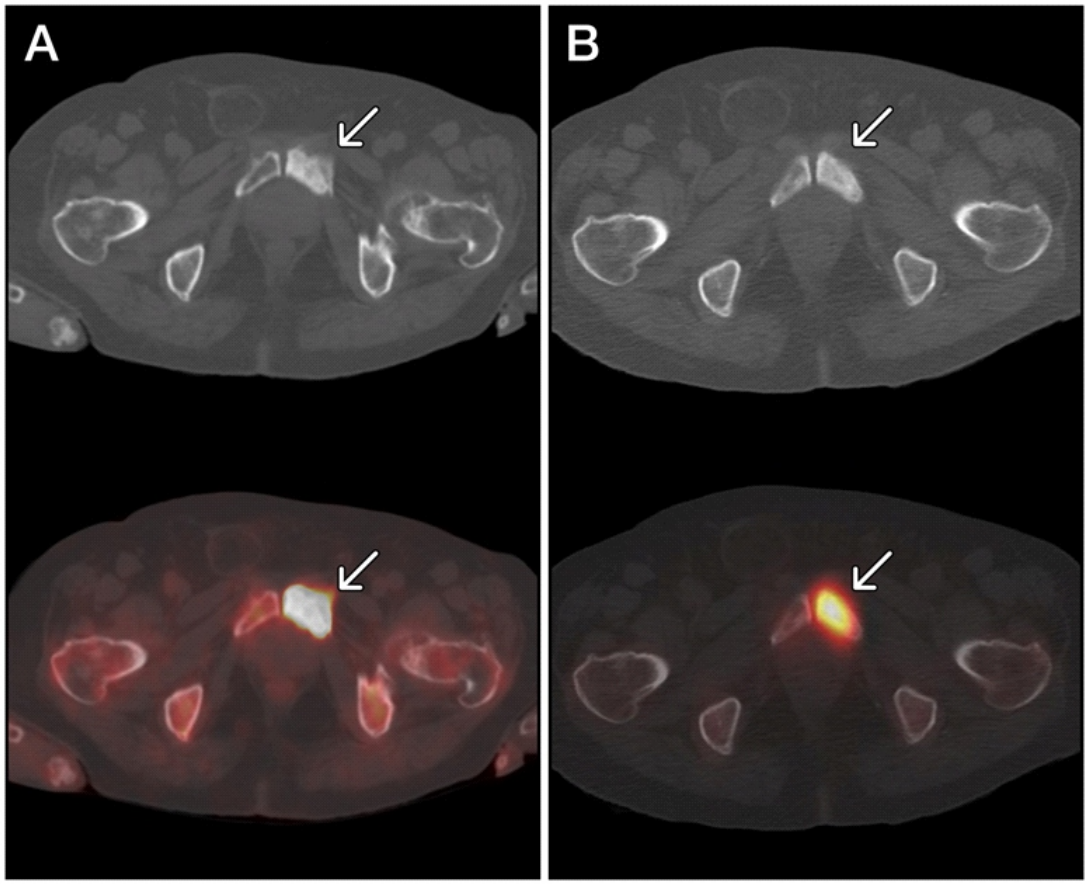


**Figure 2.** Technetium-99m-MDP SPECT/CT (A) and $^{18}$F-NaF PET/CT (B) images of a patient showing a sclerotic area of metastasis in left pubic bone, adjacent to symphisis (arrows).

The two cornerstone modalities in nuclear medicine, PET and SPECT, are widely used for staging and follow-up of various malignancies. Standardized uptake value quantification offers an objective rationale for the assessment of disease burden, response to treatment or disease progression. Quantification in PET has been the standard approach ever since the introduction of the modality into clinical practice in the early 2000s. However, SPECT assessment has worked in terms of relative counts and ratios between areas of uptake.

Historic barriers for quantitative SPECT included stability and uniformity of gamma cameras, suboptimal correction of attenuation and scatter, lack of correction for collimator-detector response, basic reconstruction algorithms and limited computing power. Today, these challenges have been mostly compensated with significant improvements in software (e.g., spatially adaptive noise reduction filters, iterative image reconstruction) and hardware (e.g., solid-state cameras, multi-pinhole collimators, better energy resolutions, improved rejection of scatter photons). In addition to these compensation steps, a careful and consistent calibration between counts and activity concentrationis needed for absolute quantification in SPECT [1, 2, 13]. Conventionally, SPECT images are represented in terms of counts per voxel. We need to convert this data from counts per voxel to Becquerels per voxel to get SUV measurements that we are familiar with from PET imaging [14]. Besides, by this data conversion, we can generate time profile of activity within a voxel or organ, which then can be used to compute the absorbed dose rate (Grays per second) and provide insights for internal dosimetry in molecular radiotherapy [15]. Mechanism to calculate SPECT sensitivity is currently available in many commercial SPECT/CT systems, which consummates the necessary equipment for the spread of quantitative SPECT [16].

By using PET and SPECT agents with similar mechanisms of uptake, we could calculate the strength of correlation between the two modalities and evaluate the performance of SPECT as a quantification tool. Technetium-99m-MDP and $^{18}$F-NaF are two different bone-seeking agents with almost the same mechanisms of skeletal uptake [17-19]. After intravenous injection, $^{99m}$Tc-MDP is taken up by bones via active transport and passive diffusion across the osteocyte cell membrane. Once inside the osteocyte, $^{99m}$Tc-MDP binds to hydroxyapatite crystals until its excretion into the interstitial fluid and eventually moves into the circulation where it is eliminated via urinary excretion. Similarly, $^{18}$F-NaF, crosses the cell membranes and gets hydrolyzed to form fluoride ions, which then combine with free calcium ions to form fluorapatite, a crystalline compound similar to hydroxyapatite. This similar mechanism of uptake for $^{99m}$Tc-MDP and $^{18}$F-NaF makes them ideal tracers for a quantitative comparison.

A review of the literature shows that there is a gradual accumulation of evidence regarding the quantification of $^{99m}$Tc-MDP SPECT/CT. Arvola et al. (2019) made a similar study design on a larger cohort of prostate and breast cancer patients, and they found an even stronger correlation ($\geq$0.80, P<0.001) between SUV of bone metastases measured in $^{99m}$Tc-hydroxy diphosphonate (HDP) SPECT/CT and $^{18}$F-NaF PET/CT [3]. The relatively weaker correlation seen in our study could have been due to smaller sample size and differences in SPECT calibration. The quantitation of SPECT is prone to the effects of many factors, including biological (e.g., scan time after injection, patient motion), technical (e.g., dose calibrator settings, extravasation of radiopharmaceutical) and scanner-specific (e.g., image reconstruction algorithms, calibration of the system) entities [20-22].

The sensitivity of SPECT SUV for distinguishing benign and malignant areas of uptake was also investigated in some recent studies. Tabotta and colleagues analyzed the SUV derived from $^{99m}$Tc-dicarboxy-propane-diphosphonate (DPD) SPECT/CT images of prostate cancer patients and showed significantly higher values of SUVmax and SUVmean in metastatic lesions when compared to osteoarthritic changes [23]. Benign and malignant lesions could be distinguished using the SUVmax cut-off of 19.5g/mL with a sensitivity and specificity of 87% and 92%, respectively, suggesting that SPECT SUV could be a useful additional technique in this setting. In a similar approach, Kuji et al. (2017) found that SUV of active bone metastases in $^{99m}$Tc-MDP SPECT/CT were greater than those for degenerative in patients with prostate cancer, with a feasible discrimination accuracy of the hot foci [24]. The authors concluded that SPECT SUV are promising indices for objectively evaluating the burden of bone metastases. Similarly, Kitajima et al. (2020-21) reported significantly higher values of SUVmax for malignant primary and cartilaginous bone neoplasms [25, 26].

The limitations of our study include its small sample size and retrospective design. Inter-observer variability for lesion segmentation was not evaluated within the context of this study. The sensitivity and specificity of SUV measurements were also not investigated since a biopsy sampling would not be clinically feasible for most bone lesions.

*In conclusion*, we found positive strong correlation between SUV metrics of osteoblastic bone metastases derived from $^{99m}$Tc-MDP SPECT/CT and $^{18}$F-NaF PET/CT studies of prostate and breast cancer patients. A novel aspect brought by this study was the assessment of correlation according to the size and localization of lesions, which revealed that larger lesions in the appendicular skeleton could demonstrate a stronger correlation. If validated with larger, multi-centric cohorts, quantification of $^{99m}$Tc-MDP SPECT/CT could be a cost-effective and accessible approach that contributes to diagnostic precision, treatment planning and objective follow-up of bone metastases.

*The authors declare that they have no conflicts of interest.*

## Bibliography


1. Bailey DL, Willowson KP. Quantitative SPECT/CT: SPECT joins PET as a quantitative imaging modality. *Eur J Nucl Med Mol Imaging* 2014; 41(1): 17-25.
2. Rosenthal M, Cullom J, Hawkins W et al. Quantitative SPECT imaging: a review and recommendations by the Focus Committee of the Society of Nuclear Medicine Computer and Instrumentation Council. *J Nucl Med* 1995; 36(8): 1489-513.
3. Arvola S, Jambor I, Kuisma A et al. Comparison of standardized uptake values between $^{99m}$Tc-HDP SPECT/CT and $^{18}$F-NaF PET/CT in bone metastases of breast and prostate cancer. *EJNMMI Res* 2019; 9(1): 6.
4. Utsunomiya D, Shiraishi S, Imuta M et al. Added value of SPECT/CT fusion in assessing suspected bone metastasis: comparison with scintigraphy alone and non fused scintigraphy and CT. *Radiol* 2006; 238(1): 264-71.

5. Alqahtani M, Fulton R, Constable C et al. Diagnostic performance of whole-body SPECT/CT in bone metastasis detection using $^{99m}$Tc-labelled diphosphate: a systematic review and meta-analysis. *Clin Radiol* 2020; 75(12): 961. e911-961. e924.
6. Shen G, Deng H, Hu S, Jia Z. Comparison of choline-PET/CT, MRI, SPECT, and bone scintigraphy in the diagnosis of bone metastases in patients with prostate cancer: a meta-analysis. *Skeletal Radiol* 2014; 43(11): 1503-13.
7. Palmedo H, Marx C, Ebert A et al. Whole-body SPECT/CT for bone scintigraphy: diagnostic value and effect on patient management in oncological patients. *Eur J Nucl Med Mol Imaging* 2014; 41(1): 59-67.
8. Zhou J, Gou Z, Wu R et al. Comparison of PSMA-PET/CT, choline-PET/CT, $^{18}$F-NaF-PET/CT, MRI, and bone scintigraphy in the diagnosis of bone metastases in patients with prostate cancer: a systematic review and meta-analysis. *Skeletal Radiol* 2019; 48(12): 1915-24.
9. Iagaru A, Mittra E, Dick DW, Gambhir SS. Prospective evaluation of $^{99m}$Tc MDP scintigraphy, $^{18}$F NaF PET/CT, and $^{18}$F-FDG PET/CT for detection of skeletal metastases. *Mol Imaging Biol* 2012; 14(2): 252-9.
10. Langsteger W, Rezaee A, Pirich C, Beheshti M. $^{18}$F-NaF-PET/CT and $^{99m}$Tc-MDP bone scintigraphy in the detection of bone metastases in prostate cancer. *Semin Nucl Med* 2016; 46(6): 491-501.
11. Dewaraja YK, Frey EC, Sgouros G et al. MIRD pamphlet No. 23: quantitative SPECT for patient-specific 3-dimensional dosimetry in internal radionuclide therapy. *J Nucl Med* 2012; 53(8):1310-25.
12. Huang K, Feng Y, Liang W et al. Impact of partial volume effect on quantitative results in SPECT/CT. *Chin J Med Imaging* 2017; 12: 867-71.
13. Bailey DL, Willowson KP. An evidence-based review of quantitative SPECT imaging and potential clinical applications. *J Nucl Med* 2013; 54(1): 83-9.
14. Ritt P, Kuwert T. Quantitative SPECT/CT-technique and clinical applications. *Recent Results Cancer Res* 2020; 216: 565-90.
15. Zanzonico PB, Bigler RE, Sgouros G, Strauss A. Quantitative SPECT in radiation dosimetry. *Semin Nucl Med* 1989;19(1): 47-61.
16. Dickson J, Ross J, Vöö S. Quantitative SPECT: the time is now. *EJNMMI Phys* 2019; 6(1):1-7.
17. Okamoto YM. Mechanism of accumulation of $^{99m}$Tc-MDP to bone: correlation of in vivo data with in vitro data. *Radiation Med*1997; 15(4): 209-15.
18. Toegel S, Hoffmann O, Wadsak W et al. Uptake of bone-seekers is solely associated with mineralisation! A study with $^{99m}$Tc-MDP, $^{153}$Sm-EDTMP and $^{18}$F-fluoride on osteoblasts. *Eur J Nucl Med Mol Imaging* 2006; 33(4): 491-4.
19. Czernin J, Satyamurthy N, Schiepers C. Molecular mechanisms of bone $^{18}$F-NaF deposition. *J Nucl Med* 2010; 51(12): 1826-9.
20. Kupitz D, Wissel H, Wuestemann J et al. Optimization of SPECT/CT imaging protocols for quantitative and qualitative $^{99m}$Tc SPECT. *EJNMMI Phys* 2021; 8(1): 57.
21. Hishikawa M, Matsutomo N, Yamamoto T. Impact of reconstruction parameters on quantitative bone SPECT imaging: A novel thoracic spine phantom study. *Hell J Nucl Med* 2019; 22 Suppl 2:140.
22. Anizan N, Wang H, Zhou XC et al. Factors affecting the stability and repeatability of gamma camera calibration for quantitative imaging applications based on a retrospective review of clinical data. *EJNMMI Res* 2014; 4(1): 67.
23. Tabotta F, Jreige M, Schaefer N et al. Quantitative bone SPECT/CT: high specificity for identification of prostate cancer bone metastases. *BMC Musculoskelet Disord* 2019; 20(1): 619.
24. Kuji I, Yamane T, Seto A et al. Skeletal standardized uptake values obtained by quantitative SPECT/CT as an osteoblastic biomarker for the discrimination of active bone metastasis in prostate cancer. *Eur J Hybrid Imaging* 2017; 1(1): 2.
25. Kitajima K, Futani H, Komoto H et al. Quantitative bone SPECT/CT applications for primary bone neoplasms. *Hell J Nucl Med* 2021; 24(1): 36-44.
26. Kitajima K, Futani H, Tsuchitani T et al. Quantitative bone SPECT/CT applications for cartilaginous bone neoplasms. *Hell J Nucl Med* 2020; 23(2): 133-7.